Development 135, 2873-2881 (2008) doi:10.1242/dev.021618

Fgf8 controls regional identity in the developing thalamus

Ayane Kataoka and Tomomi Shimogori*

The vertebrate thalamus contains multiple sensory nuclei and serves as a relay station to receive sensory information and project to corresponding cortical areas. During development, the progenitor region of the diencephalon is divided into three parts, p1, p2 (presumptive thalamus) and p3, along its longitudinal axis. Besides the local expression of signaling molecules such as sonic hedgehog (*Shh*), Wnt proteins and Fgf8, the patterning mechanisms of the thalamic nuclei are largely unknown. Using mouse in utero electroporation to overexpress or inhibit endogenous Fgf8 at the diencephalic p2/p3 border, we revealed that it affected gene expression only in the p2 region without altering overall diencephalic size or the expression of other signaling molecules. We demonstrated that two distinctive populations in p2, which can be distinguished by *Ngn2* and *Mash1* in early embryonic diencephalon, are controlled by Fgf8 activity in complementary manner. Furthermore, we found that FGF activity shifts thalamic sensory nuclei on the A/P axis in postnatal brain. Moreover, gene expression analysis demonstrated that FGF signaling shifts prethalamic nuclei in complementary manner to the thalamic shift. These findings suggest conserved roles of FGF signaling in patterning along the A/P axis in CNS, and reveal mechanisms of nucleogenesis in the developing thalamus.

KEY WORDS: Diencephalon, Thalamus, Nuclei, Homeobox genes, Shh, Fgf8, Mouse

INTRODUCTION

The patterning and growth of a particular tissue is thought to be organized by signaling molecules expressed by specialized boundary regions between tissue compartments (Tabata, 2001). The central nervous system (CNS) is a complex tissue including multiple types of neurons, which participate in elaborate neuronal circuits. Signaling molecules secreted from distinct signaling centers, which establish positional information and regulate regional growth, can allocate neuronal cell identities, as well as regional identities. For example, regional signaling centers have been shown to establish cortical area maps, midbrain nucleogenesis, dorsal ventral patterning in the spinal cord, and the compartmentalization of the diencephalon (Fukuchi-Shimogori and Grove, 2001; Agarwala et al., 2001; Chiang et al., 1996; Kiecker and Lumsden, 2004).

The thalamic region comprises three functionally distinct zones, the prethalamus, the thalamus proper and the pretectum, along the anterior-posterior (A/P) axis of the diencephalon (Figdor and Stern, 1993; Puelles and Rubenstein, 2003; Larsen et al., 2001). The thalamus has been considered as a relay center in which specific thalamic nuclei receive and project particular sets of fibers to targeted cortical fields. Sensory inputs are, in turn, transmitted to the somatosensory cortex through a relay station in the ventroposterior (VP) nucleus complex, known as the barreloid of the thalamus (Erzurumlu and Kind, 2001). By contrast, the prethalamus, which includes the reticular nucleus, zona incerta and ventral lateral geniculate nucleus (vLGN), does not send axons to cortex.

The progenitor region of diencephalon has been subdivided into transverse domains defined by morphological and molecular criteria, including p1 (the presumptive pretectum), p2 (presumptive thalamus) and p3 (presumptive prethalamus). Recent studies have established the identity of molecules that may control the patterning of the diencephalon in mice (Nakagawa and O'Leary, 2001; Nakagawa and O'Leary, 2003; Fode et al., 2000; Miyashita-Lin et al., 1999; Puelles et al., 2006; Suda et al., 2001), monkey (Jones and Rubenstein, 2004) and chick (Kobayashi et al., 2002; Lim and Golden, 2002). The zona limitans intrathalamica (ZLI), a neuroepithelial domain in the alar plate of the diencephalon, has been suggested to separate p3 from p2 (Larsen et al., 2001), and may function as a secondary organizer (Vieira et al., 2005). The expression of the signaling molecule sonic hedgehog (Shh) in ZLI is a key source of signals that pattern the thalamus in mice (Ishibashi and McMahon, 2002), chick (Kiecker and Lumsden, 2004; Lim and Golden, 2007; Vieira et al., 2005; Hashimoto-Torii et al., 2003; Zeltser, 2005) and zebrafish (Scholpp et al., 2006). Additionally, Wnt expression in thalamus is also required for normal development, especially for the establishment of regional thalamic identities (Braun et al., 2003; Zhou et al., 2004). However, the molecular and cellular mechanisms that pattern functional nuclei within each region in the diencephalon are still largely unknown.

Fibroblast growth factor 8 (Fgf8) is expressed in the dorsal part of the diencephalon, as already described in previous studies and also in the present study (Fig. 1C), though its true function in the diencephalon is largely unknown (Crossley et al., 2001). Although, Fgf8-coated bead placement in caudal diencephalon induces an ectopic midbrain/hindbrain boundary (Crossley et al., 1996), the function of endogenous Fgf8 in diencephalon has not been explored. Fgf8 is also expressed in other parts of the CNS in various animals for appropriate control of development, suggesting important roles for it in the developing diencephalon (Chi et al., 2003; Garel et al., 2003; Shanmugalingam et al., 2000; Shimamura and Rubenstein, 1997; Storm et al., 2006; Walshe and Mason, 2003; Ye et al., 1998). We explored this possibility by employing mouse in utero electroporation to manipulate Fgf8 in the developing diencephalon in a temporally and spatially restricted manner. We found that Fgf8 activity controls the patterning of thalamic nuclei and also that of some of the prethalamic nuclei on the A/P axis. However, analysis of electroporated brains in the early embryonic stage demonstrated that regional shifts due to FGF activity occur only in the p2 progenitor region. Our detailed gene analysis in the early embryonic stage suggests the identity of the progenitor regions

RIKEN Brain Science Institute, 2-1 Hirosawa, Wako-Shi, Saitama 351-0198, Japan.

*Author for correspondence (tshimogori@brain.riken.jp)

Accepted 26 June 2008

of nuclei shifted by FGF activity. These findings aid in determination of the molecular and cellular mechanisms of nucleogenesis of the diencephalon.

MATERIALS AND METHODS

Mice

Outbred ICR (CD-1) timed pregnant mice were obtained from Japan SLC. Midday of the day of vaginal plug discovery was considered to be embryonic (E) day 0.5.

In situ hybridization

For section in situ hybridization, brains were removed, fixed overnight in 30% sucrose/4% paraformaldehyde, and sectioned in a semi-horizontal plane (Fig. 2A) on a Leica sledge microtome at 40 μm. Each section was mounted on slides and hybridized to visualize expression of different gene. For whole-mount in situ hybridization, embryos are collected and fixed overnight. Each pattern of gene expression was confirmed in at least four to six replications/age. Single- or two-color non-radioactive in situ hybridization was performed using a method described previously (Grove et al., 1998), including use of the chromagens nitroblue tetrazolium (Nacalai, Japan; 350 mg/ml) and tetranitroblue tetrazolium (Research Organics; 350 mg/ml).

Fluorescent in situ hybridization

Fluorescent in situ hybridization was performed with slight modification of in situ hybridization (using a protocol kindly provided by Drs Parnaik and Ragsdale). Riboprobes incorporating digoxigenin- (DIG), fluorescein- (FL) or dinitrophenyl (DNP)-labeled nucleotides were hybridized overnight and detected with each antibody conjugated to HRP. Signals were detected using the TSA plus system (Perkin Elmer). Images were acquired with a DP30 (Olympus) camera and processed using Lumiavision software.

Electroporation

Electroporation was performed as described previously, with some modifications for electroporation of the diencephalon (Fukuchi-Shimogori and Grove, 2001). DNA solution was injected into the 3rd ventricle followed by negative electrode insertion in the lumen of the 3rd ventricle. The positive electrode was placed outside, near the head of the embryo. A series of three square-wave current pulses (7V, 100 ms) was delivered, resulting in gene transfection into one side of the diencephalic wall.

RESULTS

Fgf8 is expressed in the developing diencephalon

Prompted by the observation that Fgf8 in the anterior neural tube regulates patterning of the telencephalon, we examined in greater detail the distribution of *Fgf8* mRNA at embryonic (E) days 9.5 and E10.5 in the mouse (Fig. 1A,C). We also performed whole-mount in situ hybridization for *Shh* to visualize a well-known local signaling center in the developing diencephalon, the zona limitans intrathalamica (ZLI), at E9.5 and E10.5 (Fig. 1B,D). Compared with the strong expression of *Shh* in the basal part of the diencephalon (Fig. 1B, arrow), expression in the prospective ZLI was not observed at E9.5. However, it began to appear with the differentiation of ZLI and was found at the p2/p3 border (Fig. 1D, blue arrow). Fgf8 expression was not observed in diencephalon at E9.5 in our in situ hybridization experiments, compared with the strong expression in the rostral patterning center in the telencephalon and midbrain/hindbrain boundary (Fig. 1A, black arrow and red arrow, respectively). However, we observed dynamic expression of *Fgf8* in diencephalon at E10.5, close to the dorsal midline of p2 (Fig. 1C, green arrow) (defined as F12, in chick) (Crossley et al., 2001) as well as expression towards ZLI (Fig. 1C, orange arrow) (defined as F11 in chick) (Crossley et al., 2001). However, Shh in ZLI exhibited similar patterns of expression in chick and mouse brain, whereas Fgf8 expression in diencephalon differed between them. In both F11 and F12 in chick brains, extensive Fgf8 expression was observed

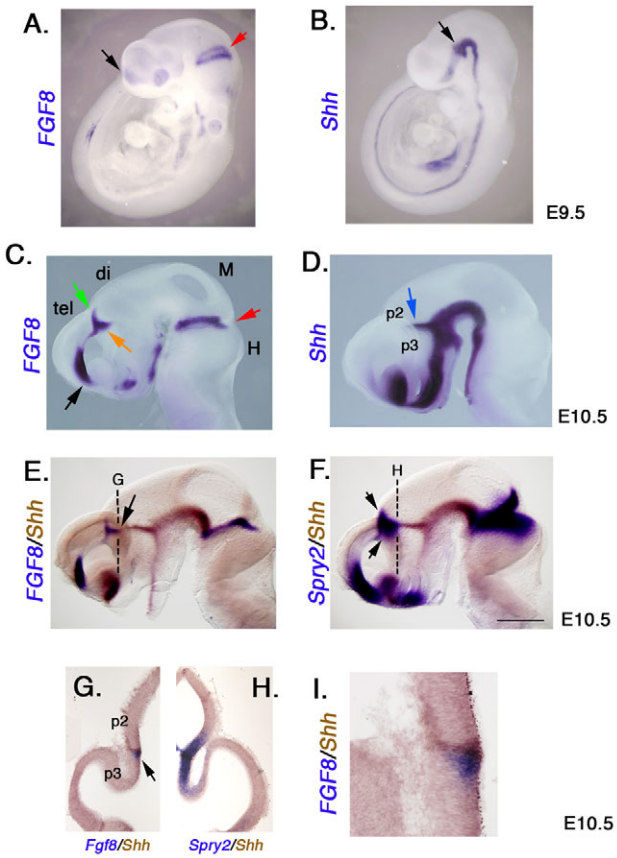

Fig. 1. Pattern of expression of Fgf8 in developing diencephalon. The spatial distribution of *Fgf8* and its activity are shown by whole-mount in situ hybridization at E9.5 in mice. Strong expression of *Fgf8* is observed at the midbrain/hindbrain boundary (MHB, red arrow) and in the anterior telencephalon (black arrow) (**A**). Strong expression of *Shh* is observed in the basal region of the diencephalon (black arrow) (**B**). (**C-F**) Whole-mount in situ hybridization of the dissected brain at E10.5 is shown. Lateral is towards the left. In addition to *Fgf8* expression in MHB and anterior telencephalon (red arrow and black arrow, respectively), expression in the dorsal part of diencephalon (green arrow) and dorsal to ZLI (orange arrow) is detected. One side of the hemisphere has been removed for a better view of *Fgf8* expression in the diencephalon (**C**). *Shh* expression in ZLI is shown (blue arrow) (**D**). Two-color in situ hybridization for *Fgf8* (blue) and *Shh* (brown) shows the spatial relationships of *Fgf8* and *Shh* expression (arrow) (**E**). FGF activity, shown by *Sprouty2* (*Spry2*, blue), is detected in both p2 and p3 (arrows), which are divided by *Shh* (brown) (**F**). (**G-I**) Section in situ hybridization shows the detailed patterns of expression of *Fgf8* and *Shh*. Estimated section positions are shown in E and F (broken line). *Fgf8* expression is restricted to p3 (arrow) (G) and a high-magnification view is shown (I). *Fgf8* activity shown by *Spry2* reached a greater distance on both sides of ZLI marked by *Shh* (H) at E10.5. di, diencephalon; H, hindbrain; M, midbrain; tel, telencephalon. Scale bar in F: 500 μm for A-F; 200 μm for G,H; 100 μm for I.

(Crossley et al., 2001), although in mouse the pattern of Fgf8 expression in both diencephalic domains was less extended (see Fig. S1A in the supplementary material). We further performed two-color in situ hybridization for direct comparison of the domains of *Fgf8* and *Shh* mRNA expression. This revealed that the *Fgf8* expression toward ZLI was exclusive and slightly anterior to *Shh* expression (Fig. 1E, arrow). However, *Spry2*, an Fgf8 target, spread on both sides of ZLI and exhibited a wider pattern of expression than *Fgf8*

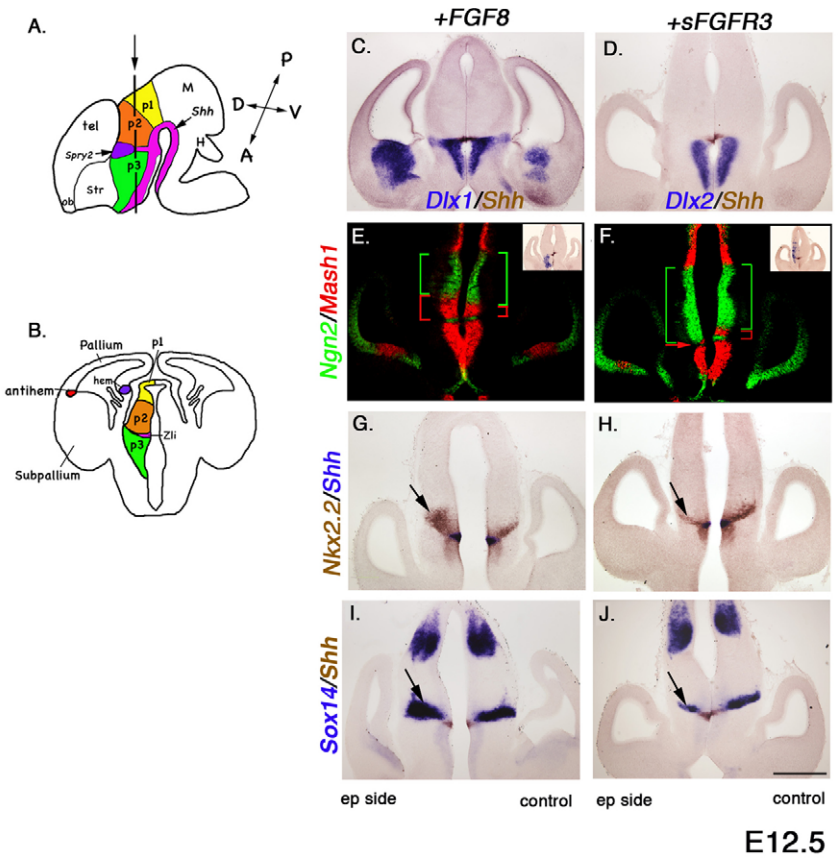

Fig. 2. Fgf8 electroporation expands the specific population posterior to ZLI in the early embryonic stage. (**A**) The selected angles of section and plane are illustrated, in sagittal view, with anterior towards the left. Brains were embedded and sectioned perpendicular to ZLI as indicated by *Shh* expression (pink). The section at the halfway point of the diencephalic tube along the D/V axis, which is also at the end of *Spry2* expression (purple) is selected (arrow). The section contains p1 (yellow), p2 (orange) and p3 (green). (**B**) Scheme of the semi-coronal section used in this study at the position indicated in A. The dorsal (pallium) and ventral (subpallium) telencephalon are divided by the cortical hem (purple) and pallium/subpallium boundary (antihem, red). The diencephalon contains p1, p2 and p3. Fgf8 and EGFP constructs are electroporated close to ZLI at E10.5 (**C,E,G,I**), and sFgfr3 and EGFP constructs are electroporated at E9.5 (**D,F,H,J**). Brains were collected at E12.5, and only those exhibiting strong EGFP fluorescence were processed for in situ hybridization. The electroporated side is to the left. No shift is observed with p3 markers *Dlx1* (C, blue) and *Dlx2* (D, blue) and the ZLI marker *Shh* (brown) in Fgf8-overexpressing (C) or -inhibited brain (D). Two-color fluorescent in situ hybridization with *Ngn2* (green) and *Mash1* (red) reveals an alternating pattern of expression in the diencephalic VZ. The *Mash1*+ Rim VZ is expanded (red bracket), whereas *Ngn2*+ VZ is shrunken (green bracket) in Fgf8-overexpressing brain (E). The site of electroporation is shown by GFP expression (blue) by in situ hybridization (inset). In Fgf8-inhibited brain, *Ngn2*+ VZ (green bracket) is expanded and *Mash1*+ Rim VZ (red arrow) is shrunken (F). *Nkx2.2* (brown), expressed in the region flanking ZLI (arrow), is expanded by Fgf8 electroporation, without expansion of *Shh* (blue) (G). A specific marker of the Rim, *Sox14* (blue), is also expanded by Fgf8 electroporation (arrow) (I). Expression of *Nkx2.2* and *Sox14* is shrunken in Fgf8-inhibited brain (H,J, arrow). Scale bar in J: 500 μm.

(Fig. 1F, arrows). The spatial relationship of the patterns of expression of *Shh* and *Fgf8* is clearly revealed in sectioned brains (Fig. 1G-I). *Fgf17* and *Fgf18*, members of the Fgf8 subfamily with similar receptor affinities and functions in other systems, are also expressed in the diencephalon in similar manner (see Fig. S1B,C in the supplementary material) (Maruoka et al., 1998), which suggests that multiple ligands might contribute to FGF activity in the developing diencephalon. Furthermore, a high level of expression of Fgf receptors was observed in diencephalon at E10.5 (see Fig. S1D-F in the supplementary material). Among three receptors (Fgfr1, Fgfr2 and Fgfr3), Fgfr1 exhibited expression only in p3, whereas both Fgfr2 and Fgfr3 exhibited a gradient of expression in p2 and p3 concentrically from the Fgf8-expressing domain in diencephalon. This also suggests the importance of Fgf activity in developing diencephalon.

Restricted expression of Fgf8 is required for correct diencephalic development

According to previous studies, thalamic nuclei are generated between E10.5 and E15.5 (Altman and Bayer, 1988). We have employed micro in utero electroporation at E10.5 unilaterally (Fukuchi-Shimogori and Grove, 2001) to overexpress Fgf8 in a spatially and temporally restricted manner. One-third of the surviving embryos with strong transgene expression throughout p2 exhibit morphology consistent with ectopic induction of midbrain (see Fig. S2A in the supplementary material, white arrow). This conversion is also suggested by the ectopic induction of *En2* expression in diencephalon (see Fig. S2C,D in the supplementary material). Another one-third of surviving embryos in each litter exhibited strong expression of transgene only in the region close to ZLI without morphological conversion of the diencephalon (see Fig. S2B in the supplementary material). We also confirmed with BrdU labeling or TUNEL assay that in these brains there is no ectopic cell growth or cell death at E13.5 (see Fig. S2E-H in the supplementary material). To test whether Fgf8 activity is restricted to around ZLI, we examined the expression of *Spry2*, the readout of Fgf8 activity, and observed increased expression close to ZLI alone (see Fig. S2I in the supplementary material, arrow). To inhibit FGF activity, we electroporated a DNA construct carrying a truncated Fgfr3 receptor (sFgfr3) described previously (Fukuchi-Shimogori and Grove, 2001; Ye et al., 1998). Electroporation was performed at E9.5, before Fgf8 is expressed (Fig. 1A), for complete suppression of Fgf8 activity. We observed decreased *Spry2* in diencephalon, suggesting successful inhibition of FGF activity by electroporation of sFgfr3 construct at E9.5 (see Fig. S2J in the supplementary material, arrow). We have also tested the effect of Fgf8 at E9.5 and detected similar effect at E10.5; however, targeting only close to the ZLI is difficult due to the size (data not shown). Furthermore, FGF inhibition at E10.5, after endogenous Fgf8 expression starts, yielded suppression of *Spry2*, though its effect was less than that produced by electroporation at E9.5 (data not shown). We therefore performed the two types of electroporation at different embryonic ages in this study: Fgf8 overexpression at E10.5 and Fgf8

inhibition at E9.5. Sites of electroporation are shown in the Fig. 2E,F; insets are hybridized with GFP probe, which has been co-electroporated with target plasmid.

Fgf8 activity alters neither Shh nor Wnt activity in diencephalon

Previous studies demonstrated that Shh activity from ZLI and Wnt activity from p2 are important in establishing regional identity in the developing diencephalon (Kiecker and Lumsden, 2004; Zhou et al., 2004; Braun et al., 2003). However, we demonstrated that expression of *Wnt3a*, *Shh* and its activity are not altered by Fgf8 overexpression (see Fig. S3A-H in the supplementary material). *Wnt8b*, which is expressed in ZLI in chick (Garcia-Lopez et al., 2004), was not detected in mouse brain at all (data not shown). These findings suggest that Fgf8 activity alters neither *Shh* nor *Wnt* expression, nor their activity. To understand the role of Fgf8 in developing diencephalon, we next tested gene expression after manipulating FGF activity in diencephalon at E12.5, when nucleogenesis takes place (Fig. 2). To visualize more clearly the A/P divisions (Figdor and Stern, 1993; Puelles and Rubenstein, 2003; Bulfone et al., 1993), we decided to section brains perpendicular to ZLI and selected a section plane around the midway point of ZLI along the D/V axis (Fig. 2A, arrow). This enables visualization of all three major regions of the diencephalon (p1, p2 and p3) in a single section (Fig. 2B).

Only tissues posterior to ZLI respond to Fgf8 activity

At E12.5, the major divisions of the diencephalon can be easily detected by the restriction of expression of some marker genes (Puelles and Rubenstein, 2003). We tested expression of these marker genes after Fgf8 overexpression or inhibition and demonstrated that the expression of the p3 markers *Dlx1* and *Dlx2* is altered by neither Fgf8 overexpression nor inhibition (Fig. 2C,D; data not shown). Nakagawa and his colleagues characterized distinctive progenitor domains in developing thalamus, which are marked by *Mash1* and *Ngn2* (Vue et al., 2007). We therefore examined the pattern of expression of *Mash1* and *Ngn2* in Fgf8-overexpressed and Fgf8-inhibited brains at E12.5 by fluorescent in situ hybridization. Surprisingly, restricted Fgf8 electroporation (Fig. 2E, inset) expanded the small *Mash1*+ population posterior to ZLI [(Fig. 2E, red bracket) defined as pTH-R in Vue et al. (Vue et al., 2007)] and resulted in concomitant reduction of *Ngn2* + VZ (Fig. 2E, green bracket). In complementary experiments, sFgfr3-electroporated brains (Fig. 2F, inset) displayed shrinkage of *Mash1* + VZ (Fig. 2F, red arrow and bracket) and expansion of *Ngn2* + VZ (Fig. 2F, green brackets). To examine how this change in gene expression in progenitor regions reflects the patterning of postmitotic cells, we further tested genes that are expressed flanking ZLI and also in postmitotic regions, such as *Nkx2.2* (Kiecker and Lumsden, 2004; Kitamura et al., 1997) and *Sox14* (Hashimoto-Torii et al., 2003). In Fgf8-overexpressed brains, *Nkx2.2*+ and *Sox14*+ populations in the postmitotic region are both expanded (Fig. 2G,I, arrow). In FGF-inhibited brains, *Nkx2.2* and *Sox14* had smaller domains of expression (Fig. 2H,J, arrow). However, control GFP electroporated brains exhibited no defects in *Nkx2.2* expression (see Fig. S4A,B in the supplementary material). Given the unique phenotypes of the populations that flank ZLI only posteriorly and are controlled by FGF signaling, we have termed this region the 'Rim (*Nkx2.2*+ and *Sox14*+)' and have determined its identity in further experiments. Furthermore, Fgf8 overexpression reduced the size not only of *Ngn2*+VZ in p2 but also the postmitotic region of p2, labeled by markers such as *Lhx9* (see Fig. S4C in the supplementary material). These findings indicate that Fgf8 activity controls only the pattern of the p2 region, which includes *Ngn2*+ VZ, the post-mitotic region in p2 and the Rim. Furthermore, diencephalic tissue exhibited responses to *Shh* electroporation that were different from responses to *Fgf8* electroporation (see Fig. S4E,F in the supplementary material). We also electroporated Shh, and found that Shh expression does not alter Fgf8 expression (data not shown), suggesting that Fgf8 has specific patterning effects in developing diencephalon restricted to p2.

The Rim is multi-complex

To determine the molecular identity of the Rim, we further investigated its gene expression signature. While searching for genes expressed in the diencephalon, we found that the homeodomain transcription factor *Six3* (Fig. 3A, arrow), the vertebrate ortholog of Aristaless (*Arx*) (Cobos et al., 2005) (Fig. 3B, arrow) and *Gad67* exhibit distinct patterns of expression in the Rim (Fig. 3C, arrow). Direct comparison of expression of *Gad67*, *Six3*, *Arx* and the Rim marker *Nkx2.2* was performed by two-color in situ hybridization and fluorescent in situ hybridization, and revealed that *Gad67* and *Six3* expression occurs in the medial region of the Rim (Fig. 3D,E, arrow and inset), while the *Arx*+ population is distinctive to the Rim (Fig. 3F, arrow and inset). We also demonstrated expression of other marker genes around ZLI, including *Tal2* (T-cell acute leukemia 2) (Bucher et al., 2000), *Pitx2* (Kitamura et al., 1997) and *Sim1* (Epstein et al., 2000) (Fig. 3G,I; data not shown). *Tal2* is expressed in the VZ of the Rim (Fig. 3G, arrow and inset), with complete overlap with *Mash1*+ Rim VZ shown on triple fluorescent in situ hybridization (Fig. 3H, arrow). *Pitx2* and *Sim1* were expressed lateral to *Shh* (Fig. 3I, arrow; data not shown). To recognize the distinct characteristics of the Pitx2- and Sim1-positive population, we termed it the 'Stream' in this study. To determine the direct spatial relationships between the *Six3*+ medial Rim, *Pitx2*+ Stream region and ZLI, we performed triple fluorescent in situ hybridization and found that these three populations exhibited no overlap in expression (Fig. 3J).

Fgf8 electroporation expands the Rim

As indicated above, we have shown that Fgf8 activity controls the size of the Rim (Fig. 2E-J). To test whether FGF activity controls only the Rim or also controls other structures, we examined specific markers around the Rim in brains electroporated with Fgf8 or sFgfr3 (Fig. 4). To focus on a restricted area, only the experimental side of the diencephalon is shown in high magnification around ZLI (with VZ on the right side). Fgf8-overexpressing brains exhibited expansion of the Rim VZ marked by *Tal2* and reduction in Fgf8-inhibited brains (Fig. 4A-C, arrows). The medial Rim, marked by *Six3* (Fig. 4D-F, green arrow) and *Gad67* (Fig. 4G-I; pink arrow), was also found to be controlled by FGF activity. However, the population posterior to ZLI but distinctive to the Rim marked by the *Arx* or *Pitx2*+ Stream was resistant to FGF activity (Fig. 4D-F, orange arrows; Fig. 4G-I, blue arrows). Taken together, these findings suggest that FGF activity in the diencephalon controls the patterning of the p2 progenitor region, which includes the Rim VZ, *Ngn2*+ VZ and medial Rim, but not the *Arx*+ and *Pitx2*+ stream regions.

Posterior vLGN and EML respond to FGF activity

To determine the effects of the shift in the progenitor region by FGF activity in the postmitotic region, we examined brains at E15.5, the earliest age at which individual thalamic nuclei can be defined by

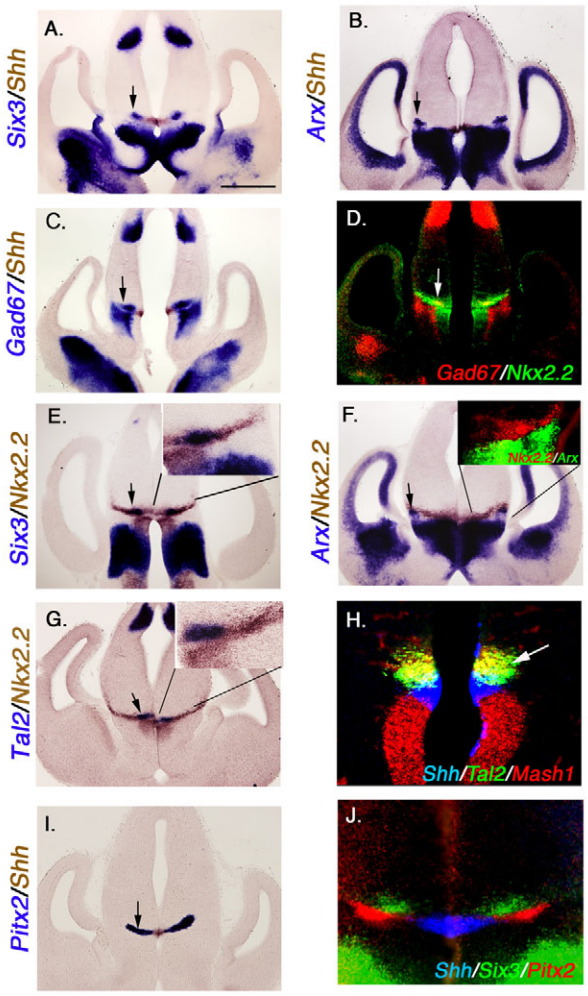

Fig. 3. Gene expression posterior to ZLI enables further subdivision. *Six3* (A), *Arx* (B) *and Gad67* (C) expression (blue) and *Shh* expression (brown) are compared at E12.5. Besides strong expression of *Six3*, *Arx* and *Gad67* in p3, there is distinctive expression of *Six3*+ close to *Shh* (**A**, arrow), *Arx*+ close to pial (**B**, arrow), and *Gad67*+ close to *Shh* (**C**, arrow). Expression of *Gad67* is observed only in the medial part of the Rim, which is marked by *Nkx2.2* shown by fluorescent in situ hybridization (**D**, arrow). *Six3* expression close to *Shh* overlaps with that of *Nkx2.2* completely (**E**, inset). No part of the *Arx* expression domain overlaps with that of *Nkx2.2* (**F**, inset). Two-color in situ hybridization of *Tal2* (blue) and *Nkx2.2* (brown) reveals that Tal2 is expressed in the Rim VZ (**G**, inset). *Tal2* expression in the Rim VZ overlaps with that of *Mash1* but not that of *Shh*, as shown by triple fluorescent in situ hybridization. A closer view of ZLI is shown (**H**). *Pitx2* (blue) is expressed lateral to *Shh* (brown) (**I**, arrow). Triple fluorescent in situ hybridization demonstrates no overlap of *Six3* (green), *Pitx2* (red) and *Shh* (blue) (**J**). Scale bar in A: 500 μm for A-G,I; 250 μm for H,I,E-G, inset.

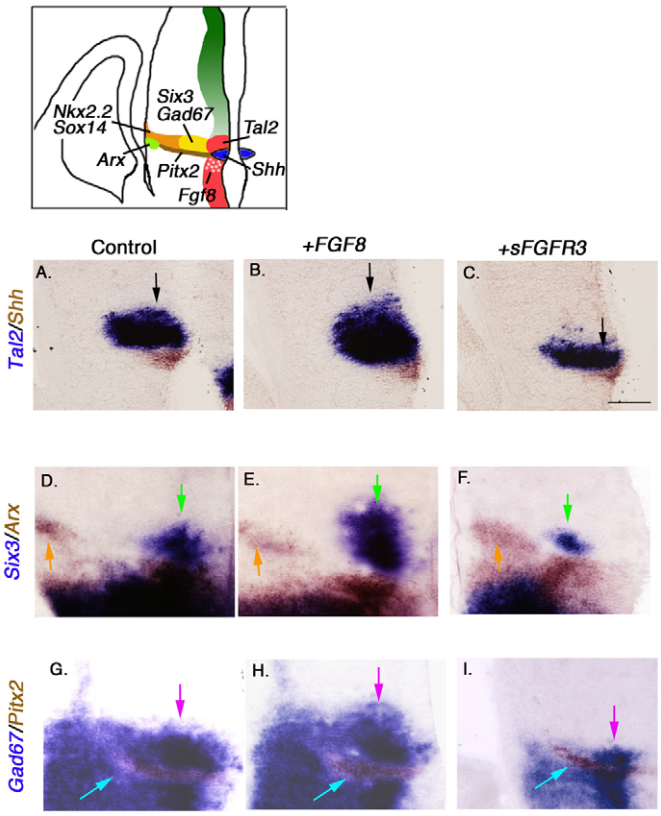

Fig. 4. Fgf8 controls the size of the Rim VZ and medial Rim. Diagram shows genes expressed around the Rim and the Stream. Electroporated brains were collected at E12.5 and examined by two-color in situ hybridization. Only the experimental side of the diencephalon is shown at high magnification around ZLI (VZ is on the right side). (**A-C**) The Rim VZ, labeled by *Tal2* (blue), is enlarged in Fgf8-overexpressing brain (B) and shrunken in Fgf8-inhibited brain (C) (black arrow), whereas *Shh* expression (brown) is unchanged. (**D-F**) The medial Rim, shown by *Six3* (blue), is enlarged in Fgf8-overexpressing brain (E) and shrunken in Fgf8-inhibited brain (F) (green arrow), while expression of *Arx* in lateral diencephalon (orange arrow) is unchanged. (**G-I**) The medial Rim, shown by *Gad67* (blue), is specifically expanded by Fgf8 electroporation and shrunken in Fgf8-inhibited brain (I) (pink arrow) while expression of *Pitx2*-labeled cells is unchanged (blue arrow). Scale bar in C: 125 μm.

gene expression patterns (Fig. 5) (Nakagawa and O'Leary, 2001). Unfortunately, we could no longer detect expression of *Tal2*, a specific marker of the Rim VZ at E15.5 with in situ hybridization (data not shown). However, examination of the Tal2-*lacZ* mouse, which contains the *lacZ* gene in the *Tal2* locus, demonstrated X-gal staining at E16.5 in the posterior part of vLGN and the external medullary lamina (EML), a structure that divides the thalamus and prethalamus in the adult (Bucher et al., 2000). This was also suggested by analysis of Mash1-EGFP transgenic mouse brain by Nakagawa and colleagues (Vue et al., 2007). However, expression of the Rim marker *Nkx2.2* and the medial Rim marker *Gad67* was detectable at E15.5, and both were expressed in posterior vLGN (Fig. 5A,B,E,F) and the EML (Fig. 5B, blue arrow). These findings suggest that the Rim might give rise to the posterior vLGN and the EML. However, *Gad67* is expressed not only in the medial Rim but also in the p3 region at E12.5 (Fig. 3C), and no *Six3* expression is detected in the posterior vLGN or EML, which make it difficult to test our hypothesis. Owing to the lack of mouse lines appropriate for true cell lineage analyses of the Rim, we further examined Fgf8-manipulated brains with these markers at E15.5 (Fig. 5C,D,G,H). In Fgf8-overexpressing brains, expansion of the posterior vLGN and a posterior shift of the EML were observed (Fig. 5C,G, arrows), while inhibition of FGF reduced the size of posterior vLGN (Fig. 5D,H, arrows). Furthermore, marker genes such as *Pitx2* and *Arx*, which did not respond to Fgf8 activity at E12.5, also exhibited no differences in expression at E15.5 compared with electroporated brains and control brains (Fig. 5B-D,F-H, yellow and green arrows,

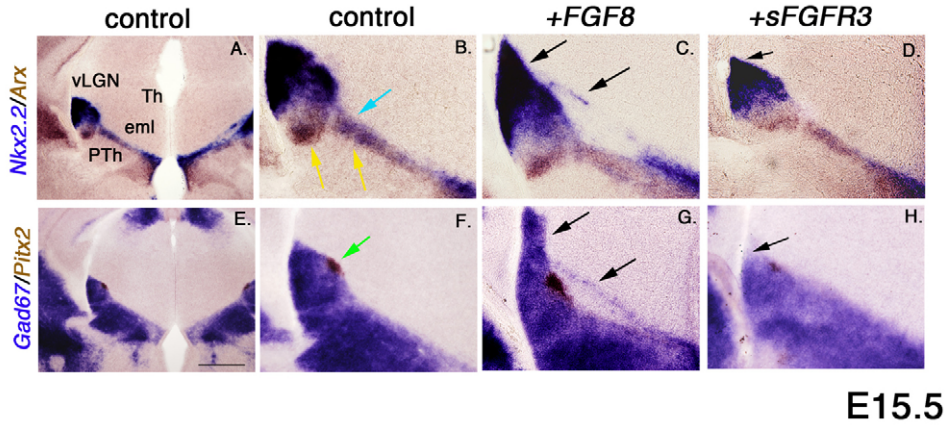

Fig. 5. Fgf8 electroporation expands the posterior vLGN and EML. Electroporated brains were collected at E15.5, sectioned coronally and examined by two-color in situ hybridization. Anterior is towards the bottom and posterior is towards the top according to the longitudinal axis (**A,E**). A closer view of vLGN and the EML region is shown (**B-D,F-H**). *Nkx2.2* (blue) marks the posterior vLGN and EML, while *Arx* (brown) marks the anterior vLGN and EML (blue and yellow arrows, respectively, B). *Gad67* (blue) labels all of PTh but not the small medial population in vLGN, which is stained by *Pitx2* (brown) (green arrow, F). The posterior vLGN is expanded posteriorly and position of posterior EML is abnormal in Fgf8-overexpressing brain (arrows in C,G) but without alteration of anterior structures labeled by *Arx* (brown staining, B,C) or the small medial population of vLGN labeled by Pitx2 (brown staining, F,G). Inhibition of Fgf8 decreased the size of the posterior vLGN (D,H, arrows), but no change was observed in the anterior vLGN (D) or *Pitx2*+ population (H). Scale bar in E: 500 μm for A,E; 200 μm for B-D,F-H.

brown staining). These findings strongly suggest that the Rim tissue that responds to FGF activity generates the posterior part of vLGN and EML.

FGF activity controls the A/P pattern of thalamic nuclei

To address our initial question of whether Fgf8 is important for the establishment of thalamic patterning, we examined the brain at postnatal (P) day 6, when the thalamic nuclei become distinguishable (Fig. 6). In rodents, somatosensory input from the whiskers on the face are transmitted to the hindbrain. Sensory inputs are in turn transmitted to the somatosensory cortex through a relay station in the ventroposterior (VP) nucleus complex, known as the barreloid of the thalamus (Erzurumlu and Kind, 2001). The Fgf8 construct was co-electroporated at E10.5 with Cre (encoding Cre recombinase) into embryos from the R26R reporter mouse line (Soriano, 1999). Expression of β-galactosidase, visualized with X-gal histochemistry, was restricted to the thalamus/prethalamus border (Fig. 6A, left side of brain). Fgf8 overexpression shifted the barreloid closer to the pretectum (posterior shift) and compressed its shape as revealed by cytochrome oxidase (CO) assay and Nissl staining (Fig. 6B,C, brackets). By contrast, blockade of FGF signaling by sFgfr3 at E9.5 reduced the size of barreloid slightly, and shifted its position closer to the prethalamus (anterior shift) (Fig.

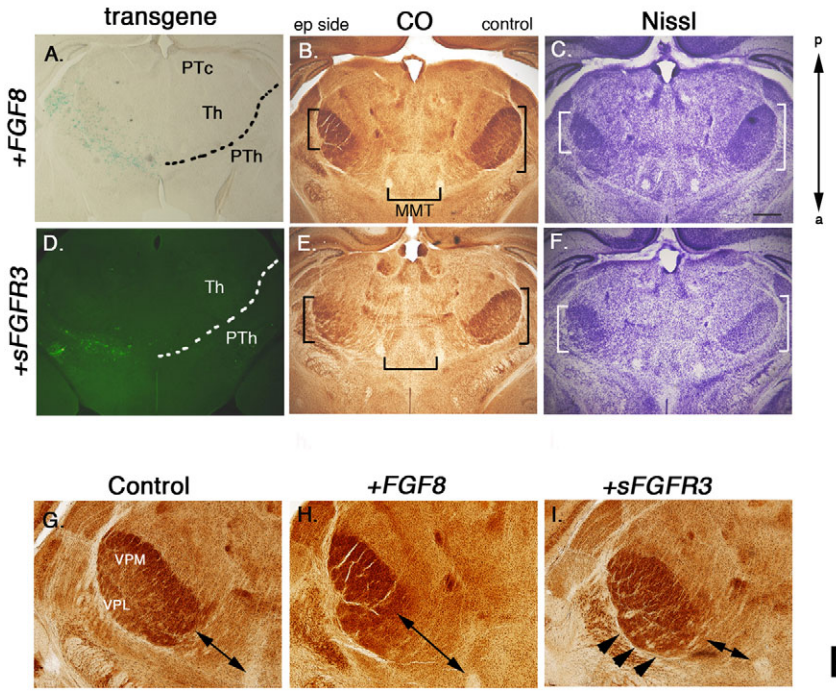

Fig. 6. Thalamic nuclei patterning is controlled by Fgf8 activity. Brains were collected at P6 and examined with X-gal histochemistry (A), cytochrome oxidase (CO) histochemistry (B,E,G-I) and Nissl staining (C,F). *Fgf8* and *Cre* constructs were co-electroporated at E10.5 into R26R mice. Brains, which have restricted staining of X-gal at the thalamus/prethalamus (Th/PTh) border (**A**), exhibit a shift of the barreloid closer to the pretectum (PTc) (**B**,**C**, bracket). Position of the mammillothalamic tract (MMT) is indicated as a landmark. *sFgfr3* and *YFP* constructs were co-electroporated at E9.5. YFP fluorescence is detectable (**D**), and brains exhibit slight anterior shift of the barreloid (**E**,**F**, bracket). (**G-I**) Higher-magnification views of VP show structural change in each brain. The ventral posterior medial (VPM) and ventral posterior lateral (VPL) subfields and their position are compared with MMT in control brain (G, double-headed arrow). Fgf8 overexpression shifts the VPM and VPL posteriorly and compresses them (H, double-headed arrow). In Fgf8-inhibited brain, VPM is closer to MML and VPL is stretched (I, double-headed arrow and arrowheads). Scale bar in C: 500 μm in A-I; 200 μm in J-L.

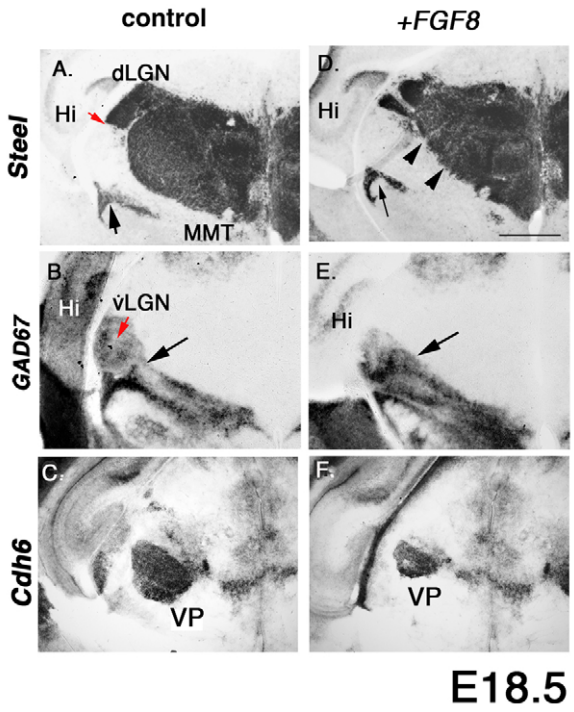

Fig. 7. Area marker genes are shifted posteriorly by Fgf8 overexpression. (**A**) *Steel* is specifically expressed in the Th and cerebral peduncle in PTh (arrow). The border of dLGN and vLGN is distinguished by *Steel* expression (red arrow). The dorsal lateral geniculate nucleus (dLGN), mammilothalamic tract (MMT) and hippocampus (Hi). (**B**) The entire PTh is labeled by *Gad67,* and structures such as vLGN are easily distinguished (red arrow). (**C**) VP is specifically labeled by *Cdh6*. (**D**) Fgf8 electroporation shifts *Steel* expression posteriorly (arrowheads). The gap between the cerebral peduncle (arrow) and *Steel*-expressing border is expanded. (**E**) The region of *Gad67* expression in PTh is enlarged in Fgf8-electroporated brain (arrow). However, it remains unclear which specific prethalamic nuclei are expanded. (**F**) Specific *Cdh6* expression is shifted posteriorly and compressed in Fgf8 electroporated brain. Scale bar in D: 0.75 mm.

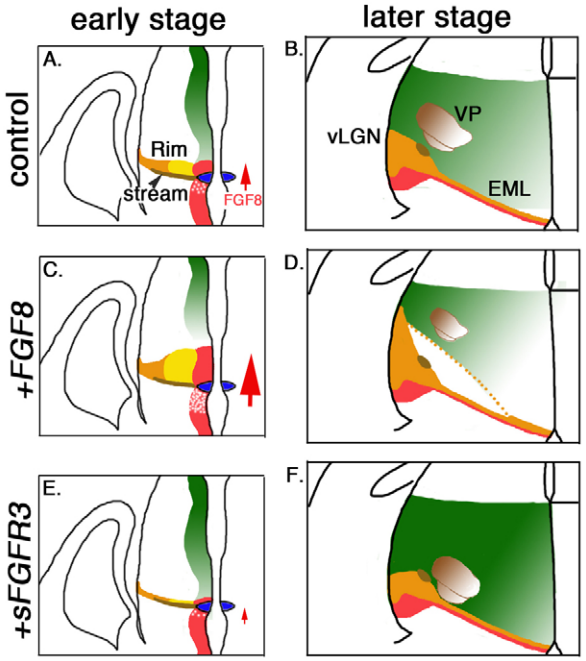

Fig. 8. Schematic representation of a model of A/P patterning of the diencephalon by Fgf8 activity.

6E,F, brackets). The site of electroporation with sFgfr3 construct is detected by YFP fluorescence (Fig. 6D). A higher-magnification view of CO assay of VP shows the shift in position of the barreloid by the distance from the MMT (mammillothalamic tract) and its structural change (Fig. 6G-I, double-headed arrow and arrowheads). These effects on patterning of Fgf8 were also examined by the expression of genes that mark specific areas of the thalamus at E18.5 (Fig. 7). Shrinkage of the thalamic region is demonstrated by *Steel* expression (Fig. 7A,D), whereas expansion of the GABAergic prethalamic region is shown by *Gad67* expression (Fig. 7B,E). Finally, *Cdh6,* which marks VP at E18.5, was also shifted posteriorly and compressed (Fig. 7C,F). In this study, we have shown that local Fgf8 expression in the diencephalon controls gene expression only in p2 (Fig. 2). However, the direct involvement of Fgf8 activity in the patterning of thalamic nuclei has not yet been demonstrated. To determine its involvement, we examined expression of the Rim marker genes and FGF activity in the early embryonic stage. At E10.5, when expression of Fgf8 begins in diencephalon (Fig. 1C), the progenitor region of p2 was already divided in two, and the Rim markers *Nkx2.2* and *Mash1* were expressed (see Fig. S5 in the supplementary material). However, Fgf8 activity did not overlap with the Rim markers along the D/V axis, suggesting that the mechanism of patterning of the Rim by FGF activity is not direct and requires downstream effectors for completion. These findings suggest that FGF activity in diencephalon controls thalamic nuclear patterning along the A/P axis, which is generated in the p2 progenitor region (Fig. 8).

DISCUSSION

Based on its morphology and gene expression, the diencephalon has been subdivided into p1-p3, which are distinct transverse compartments running along the A/P axis of the forebrain (Rubenstein et al., 1994; Puelles and Rubenstein, 2003). The only true lineage restriction in the diencephalon occurs at ZLI, which divides p2 and p3, and also exhibits expression of *Shh*. It has been suggested in previous studies that expression of signaling molecules such as Shh (Kiecker and Lumsden, 2004) and Wnt proteins (Braun et al., 2003) is important for determination of regional identity in the developing diencephalon. In our study, we focused on another signaling molecule, Fgf8, which is also locally expressed in diencephalon (Crossley et al., 2001). Fgf8 is expected to affect tissue at a distance, as it is a secreted molecule. However, expression site-dependent, tissue-specific responses were noted in our in utero Fgf8 electroporation experiments (see Fig. S2A-D in the supplementary material). When Fgf8 was specifically electroporated close to ZLI, no growth defect was observed in the diencephalon. However, when strong expression was observed in the wide p2 region, diencephalic size and morphology were dramatically altered (see Fig. S2A-D in the supplementary material). In this study, we focused on the parts of brain that receive strong Fgf8 expression close to ZLI, and demonstrated that Fgf8 controls the specific population posterior to the ZLI marked by *Nkx2.2* (Shimamura et al., 1995) and *Sox14* (Kobayashi et al., 2002), which has been defined as a Rim in this study. It has been previously reported that *Sox14* and *Nkx2.2* respond to *Shh* in dose-dependent manner (Kiecker and Lumsden, 2004; Kobayashi et al., 2002). However, our findings revealed that *Nkx2.2* and *Sox14* respond to FGF activity

without alteration of expression of *Shh* or its activity (see Fig. S3A-F in the supplementary material). Furthermore, our Shh electroporation experiments also revealed that p2 tissue responds to Shh activity but in a manner different from the response to Fgf8 (see Fig. S4E,F in the supplementary material). These findings indicate that FGF activity controls the patterning of the p2 progenitor region. Finally, the extra-toes (J) [Xt(J)] mouse mutant, which carries a deletion in the *Shh* inhibitor Gli family member Gli3, also exhibits no expansion of the Rim (A.K. and T.S., unpublished). This finding suggests that the effects of patterning by Fgf8 are independent of other signaling molecules such as Shh and Wnt proteins.

The bHLH transcription factors *Mash1* and *Ngn2* have distinct roles in specification of neurons in spinal cord and telencephalon (Parras et al., 2002; Fode et al., 2000). Interestingly, *Mash1* and *Ngn2* expression is also observed in the diencephalon at E12.5 in an alternating manner (Fig. 2E,F) (Vue et al., 2007). We have shown that *Mash1* expression in p2 overlaps with the Rim VZ marker (Fig. 3H), suggesting that the Rim contains GABAergic neurons. This is also supported by the work of Guillemot and colleagues, who showed that replacing *Ngn2* with *Mash1* leads to GABAergic differentiation of the thalamus (Fode et al., 2000). Interestingly, lack of *Otx2* causes the release of repression of *Mash1* expression in p2, which in turn causes ectopic expression of GABAergic markers in the thalamus (Puelles et al., 2006). This finding indicates that the bHLH transcription factors play important roles in determining the neuronal characteristics of the diencephalon as well. Furthermore, Martin and colleagues showed that Fgf8 represses *Otx2* expression in midbrain (Martinez et al., 1999). These finding suggests that *Mash1* upregulation in p2 by overexpression of Fgf8 is caused by repression of *Otx2*. To test this, we checked the expression of *Otx2* after Fgf8 overexpression at E12.5, and demonstrated that it represses *Otx2* expression (see Fig. S4D in the supplementary material). This finding suggests that *Mash1*+ progenitor cells for the Rim provide a GABAergic cell population posterior to ZLI, which is controlled by FGF activity via *Otx2*. To understand the role of the Rim in p2 domain in thalamic patterning, we examined the pattern of expression of the Rim marker genes at E15.5 after augmenting and reducing Fgf8 signal. When the diencephalon received excess FGF activity, posterior vLGN and the EML were expanded and shifted posteriorly (Fig. 5C,G). By contrast, these structures were specifically reduced in size in FGF-inhibited brains (Fig. 5D,H). These findings suggest that some of the prethalamic nuclei arise from the p2 domain, which is derived from the Rim. It is reported that vLGN contains several nuclei in the ground squirrel and tree shrew (Agarwala et al., 1992), but not in mouse. Further examination is required to determine which specific vLGN populations respond to FGF activity. Furthermore, a similar pattern of expression of Rim marker genes was reported in the lamprey *Lampetra fluviatilis* (Osorio et al., 2005) and in *Xenopus* brain (Bachy et al., 2001). These observations suggest that mechanisms of patterning are conserved across species in diencephalic development.

In this study, we have shown that local Fgf8 expression in the diencephalon controls gene expression on the A/P axis in p2 region (Fig. 2). This is also similar to the tissue responses of midbrain and hindbrain to Fgf8 activity in the isthmus (Liu et al., 1999). However, the Fgf8 protein and its activity appear to spread in both the p2 and p3 regions, and the mechanism of p2-specific responses to Fgf8 activity is still unclear. The ability of the tissue to respond differently to the same signaling molecule is suggested by tissue-dependent competency (Reim and Brand, 2002). Identifying the correct patterning mechanism in developing diencephalon (without loss of appropriate regional identity) will require intensive study.

We thank S. Blackshaw, C. M. Fan, T. Furuichi, F. Guillemot, M. J. Hayman, B. Hogan, K. Kitamura, G. Martin, S. L. Pfaff, D. Rowitch, J. L. Rubenstein and K. Yokota for generously providing reagents, and S. Blackshaw, S. Agarwala, C. Ragsdale, E. Grove, A. Kania, M. Yoshida, A. Suzuki-Hirano and K. Shimamura for constructive criticism of the manuscript. We also thank Y. Hamachi, A. Iida, D. Itoh, S. Kobayashi and A. Yoshida for technical support. This work was supported by the RIKEN Brain Science Institute.

Supplementary material

Supplementary material for this article is available at
http://dev.biologists.org/cgi/content/full/135/17/2873/DC1

References

Agarwala, S., May, J. G. 3rd, Moore, J. K. and Petry, H. M. (1992). Immunohistochemical organization of the ventral lateral geniculate nucleus in the ground squirrel. *J. Comp. Neurol.* **318**, 255-266.

Agarwala, S., Sanders, T. A. and Ragsdale, C. W. (2001). Sonic hedgehog control of size and shape in midbrain pattern formation. *Science* **291**, 2147-2150.

Altman, J. and Bayer, S. A. (1988). Development of the rat thalamus: III. Time and site of origin and settling pattern of neurons of the reticular nucleus. *J. Comp. Neurol.* **275**, 406-428.

Bachy, I., Vernier, P. and Retaux, S. (2001). The LIM-homeodomain gene family in the developing Xenopus brain: conservation and divergences with the mouse related to the evolution of the forebrain. *J. Neurosci.* **21**, 7620-7629.

Braun, M. M., Etheridge, A., Bernard, A., Robertson, C. P. and Roelink, H. (2003). Wnt signaling is required at distinct stages of development for the induction of the posterior forebrain. *Development* **130**, 5579-5589.

Bucher, K., Sofroniew, M. V., Pannell, R., Impey, H., Smith, A. J., Torres, E. M., Dunnett, S. B., Jin, Y., Baer, R. and Rabbitts, T. H. (2000). The T cell oncogene Tal2 is necessary for normal development of the mouse brain. *Dev. Biol.* **227**, 533-544.

Bulfone, A., Puelles, L., Porteus, M. H., Frohman, M. A., Martin, G. R. and Rubenstein, J. L. (1993). Spatially restricted expression of Dlx-1, Dlx-2 (Tes-1), Gbx-2, and Wnt-3 in the embryonic day 12.5 mouse forebrain defines potential transverse and longitudinal segmental boundaries. *J. Neurosci.* **13**, 3155-3172.

Chi, C. L., Martinez, S., Wurst, W. and Martin, G. R. (2003). The isthmic organizer signal FGF8 is required for cell survival in the prospective midbrain and cerebellum. *Development* **130**, 2633-2644.

Chiang, C., Litingtung, Y., Lee, E., Young, K. E., Corden, J. L., Westphal, H. and Beachy, P. A. (1996). Cyclopia and defective axial patterning in mice lacking Sonic Hedgehog gene function. *Nature* **383**, 407-413.

Cobos, I., Broccoli, V. and Rubenstein, J. L. (2005). The vertebrate ortholog of Aristaless is regulated by Dlx genes in the developing forebrain. *J. Comp. Neurol.* **483**, 292-303.

Crossley, P., Martinez, S. and Martin, G. R. (1996). Midbrain development induced by FGF8 in the chick embryo. *Nature* **380**, 66-68.

Crossley, P. H., Martinez, S., Ohkubo, Y. and Rubenstein, J. L. (2001). Coordinate expression of Fgf8, Otx2, Bmp4, and Shh in the rostral prosencephalon during development of the telencephalic and optic vesicles. *Neuroscience* **108**, 183-206.

Epstein, D. J., Martinu, L., Michaud, J. L., Losos, K. M., Fan, C. and Joyner, A. L. (2000). Members of the bHLH-PAS family regulate Shh transcription in forebrain regions of the mouse CNS. *Development* **127**, 4701-4709.

Erzurumlu, R. S. and Kind, P. C. (2001). Neural activity: sculptor of 'barrels' in the neocortex. *Trends Neurosci.* **24**, 589-595.

Figdor, M. C. and Stern, C. D. (1993). Segmental organization of embryonic diencephalon. *Nature* **363**, 630-634.

Fode, C., Ma, Q., Casarosa, S., Ang, S. L., Anderson, D. J. and Guillemot, F. (2000). A role for neural determination genes in specifying the dorsoventral identity of telencephalic neurons. *Genes Dev.* **14**, 67-80.

Fukuchi-Shimogori, T. and Grove, E. A. (2001). Neocortex patterning by the secreted signaling molecule FGF8. *Science* **294**, 1071-1074.

Garcia-Lopez, R., Vieira, C., Echevarria, D. and Martinez, S. (2004). Fate map of the diencephalon and the zona limitans at the 10-somites stage in chick embryos. *Dev. Biol.* **268**, 514-530.

Garel, S., Huffman, K. J. and Rubenstein, J. L. (2003). Molecular regionalization of the neocortex is disrupted in Fgf8 hypomorphic mutants. *Development* **130**, 1903-1914.

Grove, E. A., Tole, S., Limon, J., Yip, L. and Ragsdale, C. W. (1998). The hem of the embryonic cerebral cortex is defined by the expression of multiple Wnt genes and is compromised in Gli3-deficient mice. *Development* **125**, 2315-2325.

Hashimoto-Torii, K., Motoyama, J., Hui, C. C., Kuroiwa, A., Nakafuku, M. and Shimamura, K. (2003). Differential activities of Sonic hedgehog mediated by Gli transcription factors define distinct neuronal subtypes in the dorsal thalamus. *Mech. Dev.* **120**, 1097-1111.

Ishibashi, M. and McMahon, A. P. (2002). A sonic hedgehog-dependent signaling relay regulates growth of diencephalic and mesencephalic primordia in the early mouse embryo. *Development* **129**, 4807-4819.

Jones, E. G. and Rubenstein, J. L. (2004). Expression of regulatory genes during differentiation of thalamic nuclei in mouse and monkey. *J. Comp. Neurol.* **477**, 55-80.
Kiecker, C. and Lumsden, A. (2004). Hedgehog signaling from the ZLI regulates diencephalic regional identity. *Nat. Neurosci.* **11**, 1242-1249.
Kitamura, K., Miura, H., Yanazawa, M., Miyashita, T. and Kato, K. (1997). Expression patterns of Brx1 (Rieg gene), Sonic hedgehog, Nkx2.2, Dlx1 and Arx during zona limitans intrathalamica and embryonic ventral lateral geniculate nuclear formation. *Mech. Dev.* **67**, 83-96.
Kobayashi, D., Kobayashi, M., Matsumoto, K., Ogura, T., Nakafuku, M. and Shimamura, K. (2002). Early subdivisions in the neural plate define distinct competence for inductive signals. *Development* **129**, 83-93.
Larsen, C. W., Zeltser, L. M. and Lumsden, A. (2001). Boundary formation and compartition in the avian diencephalon. *J. Neurosci.* **21**, 4699-4711.
Lim, Y. and Golden, J. A. (2002). Expression pattern of cLhx2b, cZic1 and cZic3 in the developing chick diencephalon. *Mech. Dev.* **115**, 147-150.
Lim, Y. and Golden, J. A. (2007). Patterning the developing diencephalon. *Brain Res. Brain Res. Rev.* **53**, 17-26.
Liu, A., Losos, K. and Joyner, A. L. (1999). FGF8 can activate Gbx2 and transform regions of the rostral mouse brain into a hindbrain fate. *Development* **126**, 4827-4838.
Martinez, S., Crossley, P. H., Cobos, I., Rubenstein, J. L. and Martin, G. R. (1999). FGF8 induces formation of an ectopic isthmic organizer and isthmocerebellar development via a repressive effect on Otx2 expression. *Development* **126**, 1189-1200.
Maruoka, Y., Ohbayashi, N., Hoshikawa, M., Itoh, N., Hogan, B. L. and Furuta, Y. (1998). Comparison of the expression of three highly related genes, Fgf8, Fgf17 and Fgf18, in the mouse embryo. *Mech. Dev.* **74**, 175-177.
Miyashita-Lin, E. M., Hevner, R., Wassarman, K. M., Martinez, S. and Rubenstein, J. L. (1999). Early neocortical regionalization in the absence of thalamic innervation. *Science* **285**, 906-909.
Nakagawa, Y. and O'Leary, D. D. (2001). Combinatorial expression patterns of LIM-homeodomain and other regulatory genes parcellate developing thalamus. *J. Neurosci.* **21**, 2711-2725.
Nakagawa, Y. and O'Leary, D. D. (2003). Dynamic patterned expression of orphan nuclear receptor genes RORalpha and RORbeta in developing mouse forebrain. *Dev. Neurosci.* **25**, 234-244.
Osorio, J., Mazan, S. and Retaux, S. (2005). Organisation of the lamprey (Lampetra fluviatilis) embryonic brain: insights from LIM-homeodomain, Pax and hedgehog genes. *Dev. Biol.* **288**, 69-74.
Parras, C. M., Schuurmans, C., Scardigli, R., Kim, J., Anderson, D. J. and Guillemot, F. (2002). Divergent functions of the proneural genes Mash1 and Ngn2 in the specification of neuronal subtype identity. *Genes Dev.* **16**, 324-338.
Puelles, E., Acampora, D., Gogoi, R., Tuorto, F., Papalia, A., Guillemot, F., Ang, S. L. and Simeone, A. (2006). Otx2 controls identity and fate of glutamatergic progenitors of the thalamus by repressing GABAergic differentiation. *J. Neurosci.* **26**, 5955-5964.
Puelles, L. and Rubenstein, J. L. (2003). Forebrain gene expression domains and the evolving prosomeric model. *Trends Neurosci.* **26**, 469-476.
Reim, G. and Brand, M. (2002). Spiel-ohne-grenzen/pou2 mediates regional competence to respond to Fgf8 during zebrafish early neural development. *Development* **129**, 917-933.
Rubenstein, J. L., Martinez, S., Shimamura, K. and Puelles, L. (1994). The embryonic vertebrate forebrain: the prosomeric model. *Science* **266**, 578-580.
Scholpp, S., Wolf, O., Brand, M. and Lumsden, A. (2006). Hedgehog signalling from the zona limitans intrathalamica orchestrates patterning of the zebrafish diencephalon. *Development* **133**, 855-864.
Shanmugalingam, S., Houart, C., Picker, A., Reifers, F., Macdonald, R., Barth, A., Griffin, K., Brand, M. and Wilson, S. W. (2000). Ace/Fgf8 is required for forebrain commissure formation and patterning of the telencephalon. *Development* **127**, 2549-2561.
Shimamura, K. and Rubenstein, J. L. (1997). Inductive interactions direct early regionalization of the mouse forebrain. *Development* **124**, 2709-2718.
Shimamura, K., Hartigan, D. J., Martinez, S., Puelles, L. and Rubenstein, J. L. (1995). Longitudinal organization of the anterior neural plate and neural tube. *Development* **1221**, 3923-3933.
Soriano, P. (1999). Generalized lacZ expression with the ROSA26 Cre reporter strain. *Nat. Genet.* **21**, 70-71.
Storm, E. E., Garel, S., Borello, U., Hebert, J. M., Martinez, S., McConnell, S. K., Martin, G. R. and Rubenstein, J. L. (2006). Dose-dependent functions of Fgf8 in regulating telencephalic patterning centers. *Development* **133**, 1831-1844.
Suda, Y., Hossain, Z. M., Kobayashi, C., Hatano, O., Yoshida, M., Matsuo, I. and Aizawa, S. (2001). Emx2 directs the development of diencephalon in cooperation with Otx2. *Development* **128**, 2433-2450.
Tabata, T. (2001). Genetics of morphogen gradients. *Nat. Rev. Genet.* **2**, 620-630.
Vieira, C., Garda, A. L., Shimamura, K. and Martinez, S. (2005). Thalamic development induced by Shh in the chick embryo. *Dev. Biol.* **284**, 351-363.
Vue, T. Y., Aaker, J., Taniguchi, A., Kazemzadeh, C., Skidmore, J. M., Martin, D. M., Martin, J. F., Treier, M. and Nakagawa, Y. (2007). Characterization of progenitor domains in the developing mouse thalamus. *J. Comp. Neurol.* 73-91.
Walshe, J. and Mason, I. (2003). Unique and combinatorial functions of Fgf3 and Fgf8 during zebrafish forebrain development. *Development* **130**, 4337-4349.
Ye, W., Shimamura, K., Rubenstein, J. L., Hynes, M. A. and Rosenthal, A. (1998). FGF and Shh signals control dopaminergic and serotonergic cell fate in the anterior neural plate. *Cell* **93**, 755-766.
Zeltser, L. M. (2005). Shh-dependent formation of the ZLI is opposed by signals from the dorsal diencephalon. *Development* **132**, 2023-2033.
Zhou, C. J., Pinson, K. I. and Pleasure, S. J. (2004). Severe defects in dorsal thalamic development in low-density lipoprotein receptor-related protein-6 mutants. *J. Neurosci.* **24**, 7632-7639.